

Research Paper

Cite this article: Li Q, Zhang H, Lu Y, Zheng T, Lv Y (2019). A new method for path-loss modeling. *International Journal of Microwave and Wireless Technologies* **11**, 739–746. <https://doi.org/10.1017/S1759078719000084>

Received: 21 July 2018

Revised: 15 January 2019

Accepted: 16 January 2019

First published online: 22 February 2019

Key words:

Communication channels; electromagnetic propagation; fading channels; path-loss

Author for correspondence:

Hongxin Zhang, E-mail: hongxinzhang@263.net

A new method for path-loss modeling

Qiang Li¹, Hongxin Zhang^{1,2}, Yang Lu³, Tianyi Zheng¹ and Yinghua Lv¹

¹School of Electronic Engineering, Beijing University of Posts and Telecommunications, Beijing, 100876, People's Republic of China; ²Beijing Key Laboratory of Work Safety Intelligent Monitoring, Beijing, 100876, People's Republic of China and ³Global Energy Interconnection Research Institute Co., Ltd., Beijing, 102209, People's Republic of China

Abstract

In this paper, a new path-loss model for electromagnetic wave in an indoor multipath environment is proposed based on matching coefficient, polarization matching factor, and normalized field intensity direction function. This model is called the Friis-extension (Friis-EXT) model, because it operates as the Friis model under certain conditions. In addition, in the modeling process of the path-loss in an indoor environment, the reflective surfaces in the environment and form of the antenna are considered. Afterwards, the path-loss data in an indoor corridor environment are measured, and the maximum error between the theoretical value and the measured data is <7.5 dB. Finally, the Friis-EXT model is compared with some other traditional models, and the results show that the Friis-EXT model is the best one that matches the measurement data.

Introduction

In recent years, with the rapid development of the mobile Internet and popularization of the Internet of Things, the demands of communication services have grown explosively. Wireless sensor networks, as one of the core technologies of the Internet of Things, can be used in the fields of precision agriculture, logistics, smart grids, security, surveillance, habitat monitoring, health, etc. [1]. The path-loss model is an important theoretical basis for power control, link analysis, and tracking orientation in wireless sensor networks [2].

Studies on the path-loss model mainly concentrate on model parameter estimation and specific environmental modeling. In general, the path-loss types are divided into indoor models and outdoor models [3]. The indoor models include the International Telecommunications Union (ITU) model [4, 5], chan model, attenuation factor model [6, 7], one-slope model [8, 9], etc. The outdoor models include the Egli model [10, 11], Okumura model [12, 13], Hata model [14, 15], etc. In indoor rooms and corridors, there are a large number of walls; thus, the wireless signal transmission will result in reflections. Although the floor penetration loss factor is taken into account, the ITU model is not accurate enough because of neglecting the multipath effect. The chan model considers both the frequency factor and the distance factor; however, it does not consider the multipath and shadow effects. When low accuracy of indoor field strength prediction value is required, the chan model is a good choice. The attenuation factor model is very simple, and can only provide a very rough estimate of the indoor path-loss. The one-slope model is the general model that is used to compute the average path-loss without detailed knowledge of the surrounding environment. The one-slope model only takes into account the distance between the transmitting and receiving antennas. The one-slope model is applicable to free spaces or unimpeded spaces; however, its prediction error is large under complex indoor environmental conditions [16, 17]. In this paper, a new indoor path-loss model is established considering matching coefficient, polarization matching factor, normalized field intensity direction function, and wall reflection effect.

The structure of this paper is as follows. In section “Theoretical derivation”, the theory of the Friis-extension (Friis-EXT) model is introduced. In section “Measurement”, the measurement method of the wireless channel is described. In section “Result”, the proposed method is compared with traditional methods, such as the ITU model, chan model, one-slope model, and the attenuation factor model. In section “Conclusion”, the conclusion is stated.

Theoretical derivation

In the indoor multipath environment, the antenna that receives the electromagnetic wave signal can be described as follows [18].

In Fig. 1(a), the antenna receives incident electromagnetic waves from different directions in space and transmits them to the load Z_L . The area of the dotted line in Fig. 1(b) is the equivalent circuit of the receiving antenna, e_R is the electromotive force excited by external

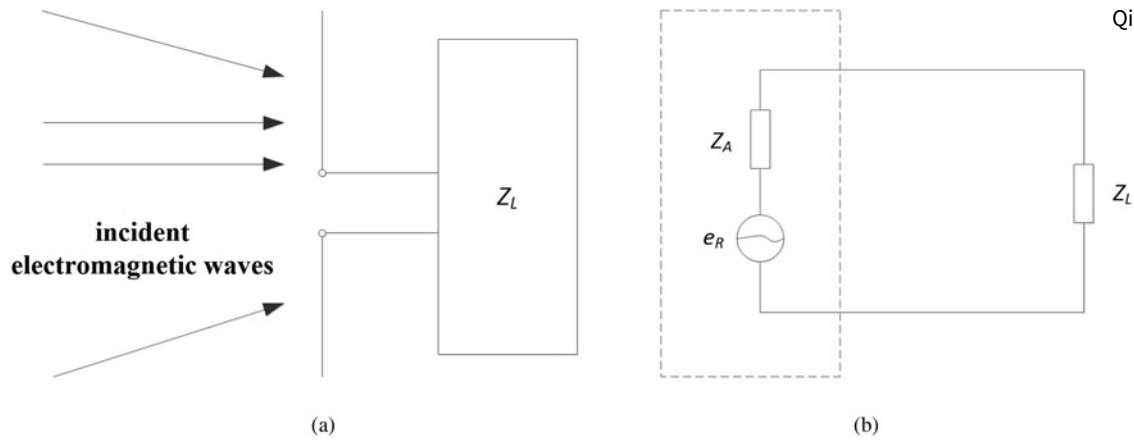


Fig. 1. Receiving antenna and equivalent circuit. (a) Receiving antenna, and (b) equivalent circuit.

electromagnetic waves on the antenna oscillator, Z_A is the internal resistance of the electromotive force, and Z_L is the load impedance of the receiving antenna.

From the equivalent circuit of the receiving antenna, we can obtain the receiving power that is transferred from the receiving antenna to the load [18].

$$P_R = \frac{1}{2} |I|^2 R_L = \frac{1}{2} \frac{e_R^2}{(R_A + R_L)^2 + (X_A + X_L)^2} \cdot R_L. \quad (1)$$

In formula (1), R_A and X_A are the input resistance and reactance of the receiving antenna, respectively, and R_L and X_L are the load resistance and reactance, respectively.

When the load and receiving antenna are conjugate matched ($Z_L = Z_A^*$), the load obtains the maximum output power, which is called the maximum receiving power P_{RM} .

$$P_{RM} = \frac{e_R^2}{8R_A}. \quad (2)$$

The relationship between the receiving power and maximum receiving power is

$$P_R = \tau P_{RM}, \quad (3)$$

where τ is called the matching coefficient, which represents the matching degree of the load and receiving antenna.

$$\tau = \frac{4R_A R_L}{(R_A + R_L)^2 + (X_A + X_L)^2}. \quad (4)$$

When the load and receiving antenna are conjugate matched, $\tau = 1$, otherwise $\tau < 1$.

If the receiving antenna undergoes a loss, $R_A = R_{\Sigma A} + R_{LA}$ ($R_{\Sigma A}$ and R_{LA} are the radiation resistance and loss resistance, respectively). Then, the maximum receiving power is

$$P_{RM} = \frac{e_R^2}{8R_{\Sigma A}} \cdot \frac{R_{\Sigma A}}{R_A} = P_{Ropt} \eta_A, \quad (5)$$

where η_A is the antenna efficiency, whose physical meaning is the ratio of radiation resistance to the total resistance of antenna, and $P_{Ropt} = e_R^2 / 8R_{\Sigma A}$ is the optimum receiving power.

According to the reciprocal theory [18],

$$e_R = \vec{E}(\theta, \phi) \cdot \vec{e} l_e F(\theta, \phi). \quad (6)$$

In formula (6), $\vec{E}(\theta, \phi)$ is an incident electric field, \vec{e} is a unit vector of antenna oscillator direction, l_e is the effective length of the receiving antenna, and $F(\theta, \phi)$ is the normalized field intensity direction function of the receiving antenna, where

$$\vec{E}(\theta, \phi) \cdot \vec{e} = E \cos(\xi). \quad (7)$$

In formula (7), E is the electric field strength value, ξ is the angle of the incoming wave electric field vector and receiving antenna oscillator. $\cos(\xi)$ is the polarization matching factor. Therefore, formula (6) can be expressed as

$$e_R = E l_e F(\theta, \phi) \cos(\xi). \quad (8)$$

The physical meaning of formula (8) is that the induced electromotive force of the receiving antenna is equal to the product of the normalized field intensity direction function of the antenna and the projection of incoming wave electric field on the effective length of the antenna oscillator. Substituting formulas (8) and (5) into formula (3), P_R can be written as

$$P_R = \frac{E^2 l_e^2 F^2(\theta, \phi)}{8R_{\Sigma A}} \cdot \eta_A \cdot \tau \cdot \cos^2(\xi). \quad (9)$$

Using the relationship between the effective length and direction coefficient [19]: $D = 30 k^2 l_e^2 / R_{\Sigma A}$, P_R can be expressed by

$$P_R = \frac{E^2 F^2(\theta, \phi)}{240k^2} \cdot D \cdot \eta_A \cdot \tau \cdot \cos^2(\xi), \quad (10)$$

where k is the wave number, which is equal to $2\pi/\lambda$, λ is the wavelength of the transmitting electromagnetic wave. The power density p and the electric field strength have the relationship [19]:

$$p = \frac{E^2}{240\pi}. \quad (11)$$

At the distance of d from the transmitting antenna, p can also be

expressed as the power of the unit sphere area with radius d .

$$p = \frac{P_T G_T}{4\pi d^2}. \tag{12}$$

In formula (12), P_T is the transmitting power, G_T is the gain of transmitting antenna, d is the distance to transmitting antenna. From formulas (11) and (12), it can be obtained as

$$E^2 = \frac{60P_T G_T}{d^2}. \tag{13}$$

By substituting formula (13) into (10), P_R can be written by

$$P_R = \frac{P_T G_T \lambda^2 F^2(\theta, \phi)}{(4\pi d)^2} \cdot D \cdot \eta_A \cdot \tau \cdot \cos^2(\xi). \tag{14}$$

Generally, the antenna gain is equal to the antenna efficiency multiplied by the directional coefficient

$$G_R = D \cdot \eta_A, \tag{15}$$

where G_R is the gain of the receiving antenna, by substituting formula (15) into formula (14), the relationship between P_R and G_R can be obtained as

$$P_R = \frac{P_T G_T \lambda^2 F^2(\theta, \phi)}{(4\pi d)^2} \cdot G_R \cdot \tau \cdot \cos^2(\xi). \tag{16}$$

When the matching coefficient τ is equal to 1, the polarization matching factor $\cos(\xi)$ is equal to 1 and the normalized field intensity direction function $F(\theta, \Phi)$ is equal to 1. Formula (16) can be expressed as

$$P_R = \frac{P_T G_T G_R \lambda^2}{(4\pi d)^2}. \tag{17}$$

Formula (17) is the Friis formula [1], and thus, we call formula (16) as Friis-EXT method. Finally, the path-loss is

$$PL = \frac{P_T}{P_R} = \frac{(4\pi d)^2}{G_T G_R \lambda^2 \tau \cos^2(\xi) F^2(\theta, \phi)}, \tag{18}$$

which is expressed in dB as

$$PL = 10[\log((4\pi d)^2) - \log(G_T) - \log(G_R) - \log(\lambda^2) - \log(\tau) - \log(\cos^2(\xi)) - \log(F^2(\theta, \phi))]. \tag{19}$$

Measurement

In this section, the indoor corridor environment is configured to conduct the measurement. The corridor is 35 m long and 3 m wide. The relative permittivity of the wall is equal to 6. The experiment scene is shown in Fig. 2(a). At the experiment site, one transmitting point and 10 receiving points are arranged to transmit and receive signals, respectively. The distance between every two adjacent points is 3 m, and the layout diagram is shown in Fig. 2(b), where the transmitting antenna is placed at the triangular point, which is 1 m above the ground. The receiving antenna is

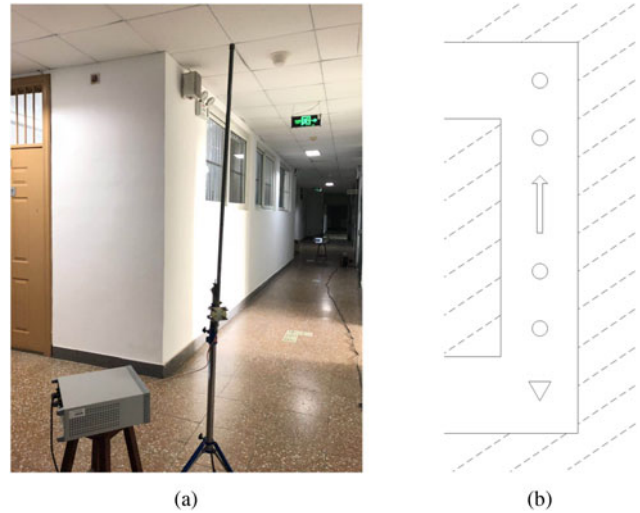


Fig. 2. Measurement layout. (a) Experiment scene, and (b) layout diagram.

placed at the circular point, of which the height is set to 0.5 and 1 m, respectively. The radio frequency signal source AV1441A produced by Ceyear and a dipole antenna TQJ-2400AT10 produced by KenBoTong are chosen as the transmitting devices, and the spectrum analyzer N1996A produced by Keysight and a dipole antenna TQJ-2400E produced by KenBoTong are chosen as the receiving devices. The radiation patterns of transmitting and receiving antennas are shown in Fig. 3. The 2.4 GHz signal is generated by the signal source with a transmitting power of 0 dBm. In the experiment, the transmitting antenna maintains vertical polarization during measurement, and the receiving antenna is set at three angles opposite the transmitting antenna, which are 0, 30, and 60°, and while the receiving antenna measures three sets of data at each height. The measurement data are shown in Tables 1–3.

Result

According to formula (19), the input parameters are set as follows. The transmitting power P_T is set as 0 dBm, the transmitting antenna gain G_T is 10 dBi, and the receiving antenna gain G_R is 3 dBi. λ is the wavelength that corresponds to the 2.4 GHz electromagnetic wave, and the impedance parameters of the receiving antenna are $R_A = 38.92 \Omega$ and $X_A = -3.64 \Omega$. The matching coefficient τ can be calculated according to formula (4). The normalized field intensity direction function $F(\theta, \Phi)$ of the receiving antenna is equal to $\sin(\theta)$. The polarization matching factor $\cos(\xi)$ can be configured by different angles. Additionally, the reflection factors are considered during the calculation. Since the field strength is weak along the axis direction of the antenna oscillator, the top and the bottom of reflective surfaces are ignored, and four reflective surfaces are considered (except the ceiling and ground). Subsequently, path-loss is obtained by superposing one direct wave and four reflected waves. The relative dielectric constant of cement is applied to calculate the reflectivity of the wall according to the formula (20):

$$\gamma_{\perp} = \left(\frac{\cos(\alpha) - \sqrt{\epsilon_2/\epsilon_1 - \sin^2(\alpha)}}{\cos(\alpha) + \sqrt{\epsilon_2/\epsilon_1 - \sin^2(\alpha)}} \right)^2, \tag{20}$$

where α is the incident angle, ϵ_1 is the relative permittivity of air, which is equal to 1, and ϵ_2 is the relative permittivity of the wall,

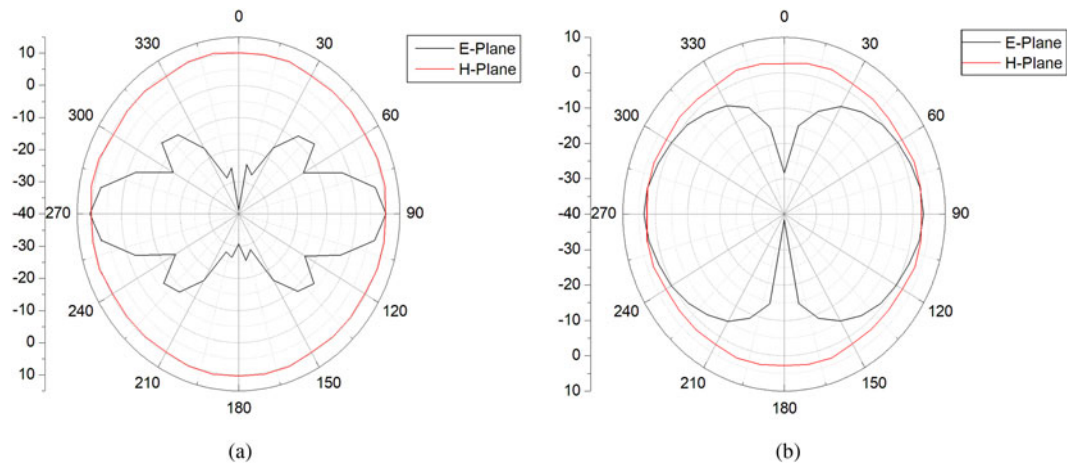


Fig. 3. Radiation patterns. (a) Transmitting antenna, and (b) receiving antenna.

Table 1. 0° angle measurement data

Distance/m	0° angle receiving power/dBm					
	0.5 m high			1 m high		
3	-46.66	-44.03	-54.89	-45.38	-45.7	-52.45
6	-54.73	-50.66	-52.56	-48.72	-46.69	-49.44
9	-52.23	-49.39	-60.33	-49.49	-54.63	-57.41
12	-56.63	-55.78	-63.22	-51.22	-58.23	-54.59
15	-58.38	-62.16	-60.75	-50.08	-57.45	-56.23
18	-63.73	-64.97	-53.91	-51.03	-59.52	-52.25
21	-62.3	-62.47	-58.78	-52.14	-57.2	-56
24	-61.55	-65.88	-64.31	-55.48	-62.88	-62.09
27	-58.17	-65.09	-67.13	-56.8	-59.16	-63.7
30	-63.31	-68.44	-63.84	-57.88	-63.02	-59.75

Table 2. 30° angle measurement data

Distance/m	30° angle receiving power/dBm					
	0.5 m high			1 m high		
3	-47.58	-56.8	-59.55	-52.34	-47.02	-50.31
6	-55.08	-59.63	-54.2	-49.13	-46.23	-50.22
9	-54.42	-67.88	-58.42	-47.64	-57.52	-62.16
12	-58.33	-62.89	-53.97	-49.41	-52.63	-57.31
15	-60.5	-67.56	-57.13	-54.13	-59.5	-63.84
18	-64.34	-73.63	-49.84	-48.31	-60.38	-62.38
21	-63.05	-61.66	-56.41	-52.41	-60.95	-68.88
24	-62.77	-66.06	-59.78	-54.22	-59.14	-63
27	-60.69	-66.44	-61.47	-55.61	-61.61	-65.84
30	-64.47	-66.09	-62.44	-56.14	-61.89	-69.75

Table 3. 60° angle measurement data

Distance/m	60° angle receiving power/dBm					
	0.5 m high			1 m high		
3	-50.61	-57.3	-62.7	-58.48	-52.17	-54.41
6	-56.61	-54.38	-51.08	-66.53	-47.52	-47.8
9	-58.2	-59.99	-74.66	-81.72	-54.13	-59.48
12	-61.61	-55.13	-63.45	-58.11	-47.97	-54.61
15	-69.97	-57.14	-66.25	-70.09	-56.02	-61.89
18	-69.22	-50.38	-61.98	-51.41	-54.91	-58.51
21	-64.31	-55.08	-72.5	-61.05	-51.94	-66.78
24	-66.94	-58.19	-63.78	-65.13	-53.69	-60.03
27	-65.59	-60.63	-79.13	-86.75	-59.11	-64.28
30	-63.06	-60.54	-74.84	-63.91	-58.94	-64.56

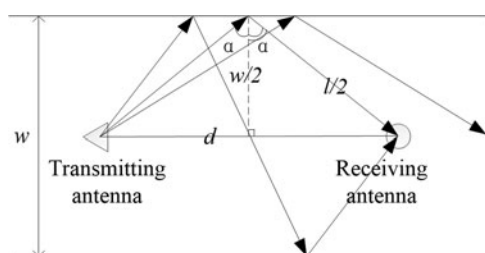


Fig. 4. Reflection path.

which is equal to 6. Formula (16) shows that the receiving power is inversely proportional to the square of the distance. The paths of the second and multiple reflections are relatively longer, and the reflectivity of the wall is calculated for each reflection, so we ignore the reflection power of the second and multiple reflections since their power is low enough to be negligible. After the electromagnetic wave is reflected by each wall, only one path can reach the receiving antenna. So the reflection point on each surface can be determined. Take one surface as an example, as shown in Fig. 4. The reflection angle is equal to the incident angle, and the test path is parallel to the corridor, so the calculation of the path distance of the reflected wave is

$$l = 2\sqrt{\left(\frac{d}{2}\right)^2 + \left(\frac{w}{2}\right)^2}, \tag{21}$$

where l is the path distance of the reflected wave, w is the corridor wide, and d is the distance between the transmitting and receiving antennas.

As shown in Fig. 5, the path-loss graph is obtained according to Friis-EXT method expressed in formula (19).

For observation, the average of three sets of the measured data is calculated at each height, respectively, and the total average of six sets of the measured data of two heights is calculated too. Figure 5(a) shows the comparison of the measured value and the predicted value of 0° polarization angle. The maximum error of 0.5 m high of receiving antenna is 2.5 dB at 15 m, and the maximum error of 1 m high of receiving antenna is 5.5 dB

at 21 m, and the maximum error between the total average and the predicted value is 2.5 dB at 21 m. Figure 5(b) shows the comparison of the measured value and the predicted value of 30° polarization angle. The maximum error of 0.5 m high of receiving antenna is 6.5 dB at 3 m, and the maximum error of 1 m high of receiving antenna is 4 dB at 12 m, and the maximum error between the total average and the predicted value is 4.5 dB at 3 m. Figure 5(c) shows the comparison of the measured value and the predicted value of 60° polarization angle. The maximum error of 0.5 m high of receiving antenna is 5 dB at 18 m, and the maximum error of 1 m high of receiving antenna is 10 dB at 18 m, and the maximum error between the total average and the predicted value is 7.5 dB at 18 m. Since the receiving antenna is artificially adjusted, the angle is not very accurate, resulting in a large deviation between the measured value of 60° and the theoretical value. In general, the theoretical values match the measured values closely. As is observed in Fig. 5, the path-loss is attenuated in accordance with the logarithmic law.

To validate the effectiveness of the proposed model, Friis-EXT method is compared with traditional methods, such as the ITU model, chan model, one-slope model, and the attenuation factor model. Since the traditional methods do not consider the polarization matching of the antennas, we use the 0° angle in the Friis-EXT model to compare with other methods. Due to the limited space, the height difference of the receiving antenna cannot be made too large, so the influence of the antenna height on the path-loss can be ignored. The average of six sets of measured data is taken for comparison. The results are shown in Fig. 6.

From Fig. 6, we observe that the differences between the traditional methods and measured data are very clear. The errors of the one-slope model, the attenuation factor model, and the ITU model are larger, and the errors of the three models between the measurement values are >10 dB at the most of measurement points. The detailed knowledge of the surrounding environment is not considered in the traditional models. The expressions are very simple, and only a rough estimate of the indoor path-loss can be provided. The Friis-EXT model takes the multipath effect into account and considers both the environmental factor and the equipment factor. The measured data are distributed on the upper and lower sides of the curve of the Friis-EXT model.

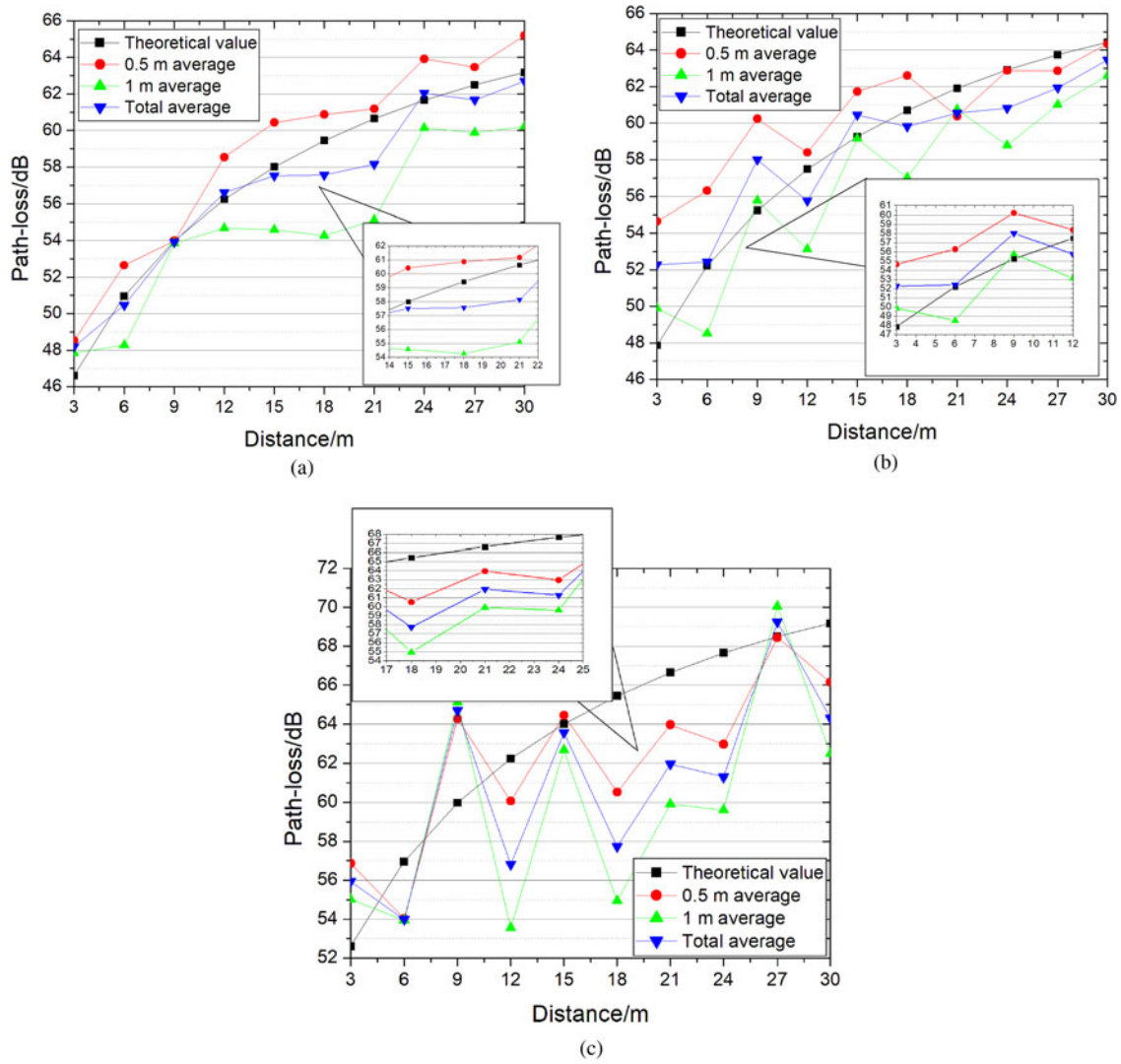


Fig. 5. Comparison of the theoretical and measured values at different polarization angles. (a) 0° polarization angle, (b) 30° polarization angle, and (c) 60° polarization angle.

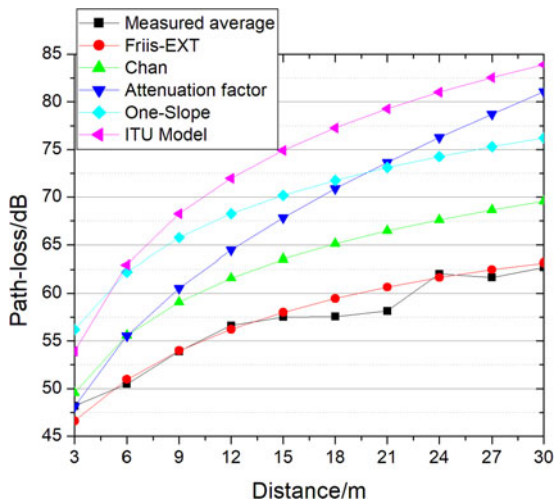


Fig. 6. Comparison of different models.

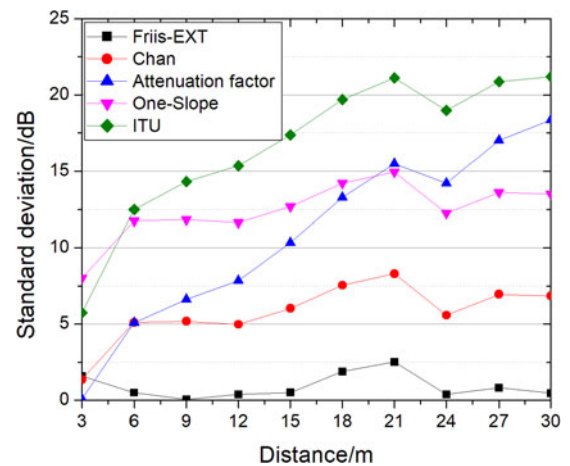



Fig. 7. The standard deviation of different models.

The standard deviation is used to judge which model can better predict the path-loss. The result is shown in Figure 7.

At each measurement point, the degree of deviation between the predicted value and the measured data is determined by solving the standard deviations of each model and measured data. Smaller standard deviation means less error, which reflects the accuracy of the model. From Figure 7, it can be realized that the standard deviation of Friis-EXT is the smallest, the Friis-EXT model is the best of these models and is a 5 dB improvement over the channel model at the most of measurement points except 3 m one.

Conclusion

A new path-loss model for an indoor multipath environment was proposed in this paper. The matching coefficient, polarization matching factor, and normalized field intensity direction function were considered in the modeling. When the matching coefficient τ , polarization matching factor $\cos(\xi)$, and normalized field intensity direction function $F(\theta, \Phi)$ are equal to 1, the formula is consistent with Friis formula. In addition, reflective surfaces were added in the calculation process, and the specific environment and form of the antenna were considered. Furthermore, the data in the indoor corridor environment were measured, with antenna set at 0, 30, and 60° angles between the transmitting and receiving antennas. The errors were <7.5 dB. Finally, the Friis-EXT was compared with other traditional models. The results show that the Friis-EXT model matched the measured data best.

Author ORCID.  Qiang Li, 0000-0003-2969-7844

Acknowledgements. The work was supported in part by the National Natural Science Foundation of China (No.61571063), and the Natural Science Foundation of Beijing Municipality (No.3182028), and the Science and technology project of State Grid Corporation of China (SGCC): Research and Chip Development of Broadband Power Line Carrier and Wireless Fusion Communication Technology.

Supplementary material. The supplementary material for this article can be found at <https://doi.org/10.1017/S1759078719000084>.

References

1. Kurt S and Tavli B (2017) Path-loss modeling for wireless sensor networks: a review of models and comparative evaluations. *IEEE Antennas and Propagation Magazine* **59**, 18–37.
2. Xu H, Zhang W and Yang Y (2016) Channel measurement and modeling for the 15 GHz radio band in an indoor corridor environment. *Journal of Communications and Information Networks* **1**, 102–108.
3. Degli-Esposti V, Vitucci EM and Martin R (2017) A simple and versatile field prediction model for indoor and indoor-to-outdoor propagation. *IEEE Access* **5**, 13270–13276.
4. Rama Rao T, Balachander D, Nishesh T and Prasad MVS N (2014) Near ground path gain measurements at 433/868/915/2400 MHz in indoor corridor for wireless sensor networks. *Telecommunication Systems* **56**, 347–355.
5. Ata OW, Shahateet AM, Jawadeh MI and Amro AI (2013) An indoor propagation model based on a novel multi wall attenuation loss formula at frequencies 900 MHz and 2.4 GHz. *Wireless Personal Communications* **69**, 23–36.
6. Seidel S and Rappaport T (1992) 914 MHz path loss prediction models for indoor wireless communications in multifloored buildings. *IEEE Transactions on Antennas and Propagation* **40**, 207–217.

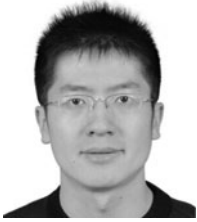
7. Xu D, Zhang J, Gao X, Zhang P and Wu Y (2007) Indoor Office Propagation Measurements and Path Loss Models at 5.25 GHz. 2007 IEEE 66th Vehicular Technology Conference, Baltimore, MD, USA, 30 September–3 October 2007, pp. 1–5.
8. Rappaport TS and McGillem CD (1989) UHF fading in factories. *IEEE Journal on Selected Areas in Communications* **7**, 40–48.
9. Ai Y, Cheffena M and Li Q (2015) Radio Frequency Measurements and Capacity Analysis for Industrial Indoor Environments. 2015 9th European Conference on Antennas and Propagation (EuCAP), Lisbon, Portugal, 13–17 April 2015, pp. 1–5.
10. Egli JJ (1957) Radio propagation above 40 MC over irregular terrain. *Proceedings of the IRE* **45**, 1383–1391.
11. Joshi GG, Dietrich Jr. CB, Anderson CR, Newhall WG, Davis WA, Isaacs J and Barnett G (2005) Near-ground channel measurements over line-of-sight and forested paths. *IEE Proceedings Microwaves, Antennas and Propagation* **152**, 589–596.
12. Okumura Y, Ohmori E, Kawano T and Fukua K (1968) Field strength and its variability in UHF and VHF land-mobile radio service. *Review of the Electrical Communication Laboratory* **16**, 825.
13. Katiyar D and Mittal V (2014) Implementation of cellular propagation models in diverse environments. *International Journal of Engineering Trends and Technology (IJETT)* **15**, 1–6.
14. Hata M (1980) Empirical formula for propagation loss in land mobile radio services. *IEEE Transactions on Vehicular Technology* **29**, 317–325.
15. Daisy G, Zheng Q and Magdy IF (2017) Path loss characteristics in urban environments using ray-tracing methods. *IEEE Antennas and Wireless Propagation Letters* **16**, 3063–3066.
16. Wang D, Song L, Kong X and Zhang Z (2012) Near-ground path loss measurements and modeling for wireless sensor networks at 2.4 GHz. *International Journal of Distributed Sensor Networks* **2012**, 1–10.
17. Hamzah SA, Baharudin MF, Shah NM, Zainal Abidin Z and Ubin A (2006) Indoor channel prediction and measurement for wireless local area network (WLAN) system. 2006 International Conference on Communication Technology, Guilin, China, 27–30 November 2006, pp. 1–5.
18. Ma H (1997) *Antenna Technology*. Harbin, China: Harbin Institute of Technology Press, pp. 17–20. (In Chinese).
19. Song Z, Zhang J and Huang Y (2003) *Antennas and Radio Wave Propagation*. Xi'an, China: Xi'an University of Electronic Science and Technology Press, pp. 10–15. (In Chinese).



Qiang Li (1985–), male, was born in Yingkou city of Liaoning province, China. He has received B.S. degree in communications engineering and M.S. degree in signal and information processing from Tianjin University of Technology and education in 2009 and 2012, respectively. Currently, he is working toward the Ph.D. degree in electronic science and technology at the Beijing University of Posts and Telecommunications. His recent research interests include electromagnetic compatibility and microwave technology, communications and signal processing. Email: qiang_lee@126.com



Hongxin Zhang (1969–), male, was born in Binzhou city of Shandong province, China. Ph.D. professor, graduated from Beijing University of Posts and Telecommunications in 2004, and received Ph.D. degree, now he works as doctoral tutor in Beijing University of Posts and Telecommunications, and director of the center for broadband communications and microwave technology. Research direction: wireless communication and electromagnetic compatibility, communication signal processing, electromagnetic radiation, information security, biomedical engineering, etc. Email: hongxinzhang@263.net



Yang Lu (1984–), male, was born in Xuzhou city of Jiangsu province, China. He graduated from Beijing University of Posts and Telecommunications in 2012, and received the Ph.D. degree, now he works as an engineer in Global Energy Internet Research Institute. Mainly engaged in research work on new technologies for power communication. E-mail: luyang@geiri.sgcc.com.cn



Tianyi Zheng (1994–), female, was born in Beijing city of China. She has received her B.S. degree from Beijing University of Technology in 2016. Currently, she is pursuing M.S. in Beijing University of Posts and Telecommunications. She completed her B.S. in electronic engineering. Research direction: wireless communication, biomedical engineering. Email: zhengtianyi@bupt.edu.cn



Yinghua Lv (1944–), male, was born in Jinzhou city of Liaoning province, China. Ph.D. professor, graduated from Beijing University of Posts and Telecommunications in 1988, and received the Ph.D. degree, now he works as a doctoral tutor in Beijing University of Post and Telecommunications. Research fields are computational electromagnetics, electromagnetic compatibility, biomedical engineering, antenna and the electromagnetic scattering, computer information technology, etc. Email: yhlu@bupt.edu.cn